International Journal of Electrical, Electronic and Communication Sciences
ISSN: 2517-9438
Vol:13, No:4, 2019

# Design and Performance Analysis of a Hydro-Power Rim-Driven Superconducting Synchronous Generator

A. Hassannia, S. Ramezani

***Abstract*****—**The technology of superconductivity has developed in many power system devices such as transmission cable, transformer, current limiter, motor and generator. Superconducting wires can carry high density current without loss, which is the capability that is used to design the compact, lightweight and more efficient electrical machines. Superconducting motors have found applications in marine and air propulsion systems as well as superconducting generators are considered in low power hydraulic and wind generators. This paper presents a rim-driven superconducting synchronous generator for hydraulic power plant. The rim-driven concept improves the performance of hydro turbine. Furthermore, high magnetic field that is produced by superconducting windings allows replacing the rotor core. As a consequent, the volume and weight of the machine is decreased significantly. In this paper, a 1 MW coreless rim-driven superconducting synchronous generator is designed. Main performance characteristics of the proposed machine are then evaluated using finite elements method and compared to an ordinary similar size synchronous generator.

***Keywords*****—**Coreless machine, electrical machine design, hydraulic generator, rim-driven machine, superconducting generator.

## I. Introduction

SUPERCONDUCTIVITY is the phenomenon of certain materials exhibiting zero electrical resistance below a critical temperature, which was first observed in 1911. The superconductivity theory is developed as well as the critical current of new high temperature superconducting (HTS) materials is increased up to 130 K in recent years. These developments have extended the applications of superconductivity in power system and many other industries. Nowadays, superconducting transmission cables, power transformers, energy storages, current limiters, motors and generators are developing in modern power systems.

The superconducting machines are compact, lightweight, and more efficient in comparison with ordinary machines. This is due to the capability of HTS coils in carrying high density electrical current without loss. Furthermore, the machine weight and size may be reduced significantly by magnetic core removal, which is possible due to the very high magnetic field that is produced by a compact HTS coil. The HTS materials and coils have been used in different structure of electrical machines such as induction machine [1], synchronous machine [2], brushless machine [3], hysteresis motor [4] and homopolar motor.

In this paper, a superconducting low speed synchronous generator is designed for a hydraulic power plant. The rim-driven structure is selected for designing of this generator, which is the structure that improves the hydrodynamic performance of the system and has not yet been used in superconducting generators. Furthermore, a part of rotor magnetic core is replaced with nonmagnetic material in order to reduce the size and weight of the generator. The electromagnetic performance of proposed structure is evaluated using finite elements method (FEM) and general specifications of the generator are compared to an ordinary similar size generator.

## II. General Structure of the Machine

The HTS synchronous generators have developed in recent decade. One of the basic types of these machines was designed by Siemens Co. in 2002 and was built in 2005 [5]. Later on, a 5-MW, 40 kV HTS synchronous generator was tested in Russia [6]. The HTS generator recently developed in wind power plant [7]. These generators usually consist of a salient pole or round rotor with HTS excitation coils. Since, the HTS excitation coils can provide a rather high ampere-turn, the air gap can be larger than conventional machine. Therefore, the stator teeth of HTS machine are usually removed to reduce the stator core loss. On the other hand, the performance of HTS wire is affected by alternative current. Thus, the HTS coils are not proper choice for stator winding. Generally, the HTS rotor and slotless ordinary stator is the conventional structure of HTS synchronous machines [8]-[10].

The coreless structure of HTS synchronous machines is recently attained [11]. Although the HTS coils can provide enough flux density in high reluctance circuit, the flux guiding in desired path is a major problem of coreless machines. In this issue, using of flux diverters is the much routine approach.

In the present paper, a salient pole iron free rotor core with HTS excitation coils, beside a slotless copper winding stator is used to design a 1-MW, 300 rpm HTS synchronous generator for a hydraulic power plant. A nonmagnetic core is used to provide the mechanical support of rotor winding, which is lighter and smaller than an iron core. Furthermore, a U-shape flux diverter is conceived around each HTS coil to decrease the perpendicular component of flux density on HTS coil. The flux diverter is also containing the cooling pipes as shown in Fig. 1.

The rim-driven machine is a modern structure of electrical machines in which the turbine placed inside the rotor core and the machine is embedded in a thin duct around the turbine.

A. Hassannia is with the Faculty of Electrical and Robotic Engineering, Shahrood University of Technology, Shahrood, Iran (corresponding author, phone: (+98) (9155334296); fax: 23-3230-0250; e-mail: amir.hassannia@shahroodut.ac.ir).

S. Ramezani is with the Moghan Cable University, Shahrood, Iran (e-mail: saharamezani@gmail.com).

Fig. 2 shows a general scheme of a rim-driven PM synchronous machine [12].

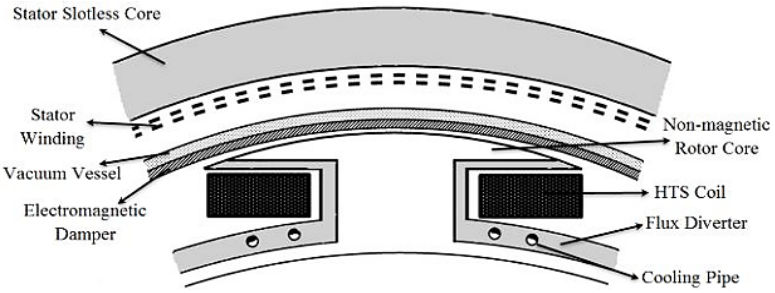


Fig. 1 General structure of new machine

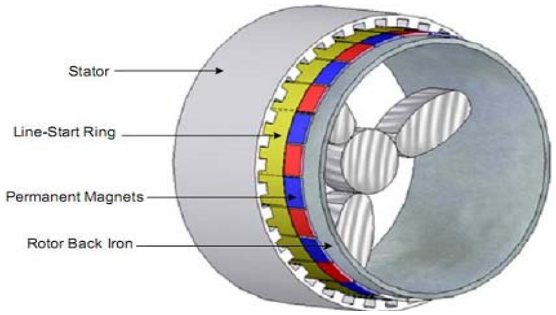


Fig. 2 General scheme of a rim-driven machine

Several types of electrical machine have made in the form of rim-driven machines such as PM synchronous [13], brushless DC [14], induction [15], and axial flux machines [16]. However, only few works have been reported dealing with superconducting rim-driven motor [17] for propulsion system application. The superconducting rim-driven hydraulic generator is a new case that is presented in this paper.

Designing of a rim-driven machine involves some problems [18]. Inner diameter of the rotor is given uniquely by outer diameter of the turbine [19]. The rim driven generator is placed in contact with fluid flow. So, in order to reduce the water drag force, the radial thickness of the machine should be minimized [20]. Furthermore, due to hydrodynamic problems, the axial length of the generator is limited to 1.5 times larger than turbine length [13]. These limitations with those are raised from the HTS coils requirements such as cooling system, maximum perpendicular flux density, and etc. should be considered in design algorithm.

## III. Design Algorithm

The mentioned limitations for a rim-driven machine are a bit more difficult for an HTS machine. Generally, the radial thickness of superconducting machine is large due to rather large air gap. Therefore, it is somewhat difficult to design an enough thin HTS machine, which can be embedded in a thin duct.

Here, a 1-MW, 300 rpm Kaplan turbine is selected as case study [20]. The main specifications of the turbine are shown in Table I. The rim-driven HTS generator should be matched with the case study turbine.

### *A. Arbitrary Parameters*

The working temperature of HTS coils ($t_w$) is the first arbitrary parameter of superconducting machines. Here, the liquid nitrogen is selected as cooling fluid. Since the boiling point of this fluid is 77 K, the working temperature is selected with a safety margin as $t_w = 75$ K.

Electrical loading factor ($ac$) and air gap flux density ($B_{ag}$) are the most effective arbitrary parameters in machine weight and size. Larger values of these parameters can provide a smaller size machine. On the other hand, although the active volume of the machine is decreased by increasing the above parameters, the machine axial length is increased by any increment of electrical loading factor or air gap flux density. This can be related to the existing complications in the structure of the rim-driven HTS machine compelling some cautions when assigning values to $B_{ag}$ and $ac$ particularly when the purpose is to obtain a thin and compact machine. The value of air gap flux density is finally selected as $B_{ag} = 0.9$ T via a reasonable trade off. Assigning the value of electrical loading factor needs more care. This parameter is defined as:

$$ac = \frac{Z \cdot I_{con}}{\pi \cdot D_{is}} \tag{1}$$

where $Z$ is total number of conductors of the stator winding, $I_{con}$ is the current of each conductor, and $D_{is}$ is inner diameter of the stator.

TABLE I
Main Parameters of Case Study Turbine

| Parameters | Values | Unit |
|---|---|---|
| Rated power | 1 | MW |
| Effective line voltage | 400 | V |
| Frequency | 50 | Hz |
| Rated speed | 300 | rpm |
| Rotor inner radius | 800 | mm |

Since the number of turns of the winding in series is related to the number of slots per pole per phase proportionally, the electrical loading factor can be chosen among some individual values within a limited band ($ac_l < ac < ac_u$). Here, the initial value of electrical loading factor is selected as $ac_0 = 50000$ A/m and its value is adjusted by an iterative loop as shown in Fig. 3. In this figure, $m$ is the number of phases, $N_{ph}$ is the number of turns of each phase, and $I_{ph}$ is the phase current. The final value of electrical loading factor that was obtained by this algorithm for the case study machine is $ac = 48322$ A/m.

*B. Air gap Design*

The air gap of superconducting machine contains of an electromagnetic damper shield, vacuum vessel isolation layer, and slotless stator winding. The thickness of damper shield is selected as %80 of magnetic penetration depth ($\delta_{thk}$), which is calculated as [21]:

$$d_{damp} = 0.8 \times \delta_{thk} = \frac{0.8}{\sqrt{\pi \mu f \sigma K_T}} \tag{2}$$

where $\mu$ is the magnetic permeability, $\sigma$ is the electric conductivity at room temperature, and $f$ is the stator frequency. Parameter $K_T$ represents the thermal correction factor that is calculated as [18]:

$$K_T = \frac{234 + t_0}{234 + t_w} \tag{3}$$

where $t_0 = 293$ K is the room temperature. The thickness of vacuum vessel and air spaces are selected typically [22].

*C. Rotor Design*

The number of poles of rotor is selected as $p = 20$ considering the generator rated speed and frequency. An iron free core provides the mechanical support for other parts of rotor as shown in Fig. 1. The thickness of rotor core is selected typically as certain percentage of turbine radius. The pole pitch angle ($\theta_p$) and rotor body angle ($\theta_{tp}$) are then calculated as:

$$\begin{aligned} \theta_p &= \frac{2\pi}{p} = 0.314 \quad rad \\ \theta_{tp} &= 0.46\, \theta_p = 0.144 \quad rad \end{aligned} \tag{4}$$

The ratio of rotor body angle to pole pitch angle is selected via a care tradeoff between field winding space and machine radial thickness. The pole height is calculated by an internal loop, which is started by estimating the pole body flux density according the following equation.

$$B_{tp} = \frac{2}{\pi} B_{ag} \left( \frac{\theta_p \cdot R_{is}}{t_p (1 - k_{leak})} \right) \tag{5}$$

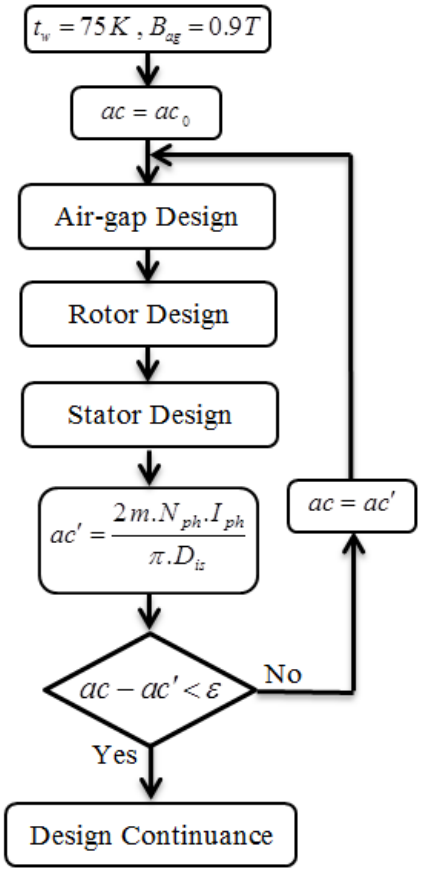


Fig. 3. Flowchart of $ac$ adjusting algorithm

where $R_{is}$ is the inner radius of stator yoke and $t_p$ is the pole body arc. Parameter $k_{leak}$ represents the leakage flux factor, which was estimated as:

$$k_{leak} = 1 - \frac{\varphi_{st}}{\varphi_r} \approx 0.09 \tag{6}$$

where $\varphi_{st}$ and $\varphi_r$ are the maximum flux in stator and rotor yoke respectively. This parameter should be investigated by finite elements method at the end of design procedure.

The magnetic reluctance of linkage flux path is then approximated and accordingly the required magneto motive force per pole is calculated as:

$$N_f I_f = (1 - k_{leak}) \varphi_{tp} \Re_g = \frac{(1 - k_{leak}) B_{tp} t_p (Ag + h_{pol} + R_{ir} \theta_p)}{\mu_0 \left( \frac{\theta_p + \theta_{tp}}{2} \right) \left( R_{is} - \frac{Ag}{2} \right)} \tag{7}$$

where $\varphi_{tp}$ is the pole body flux, $\Re_g$ is the air path reluctance, $Ag$ is the air gap, $h_{pol}$ is the pole height, and $R_{ir}$ is the rotor inner radius.

The rated current of field winding is selected according to HTS wire specifications. Here, the Superpower-SCS3050 HTS wire is selected for HTS coils of field winding. The wire specifications and its general structure are shown in Table II and Fig. 4, respectively [23].

According to Table II, the maximum allowable current value of the superconducting wire is 75 A at 77 K and zero magnetic field. As shown in Fig. 5, the HTS wire critical current is decreased by the perpendicular flux density increment [24]. If the maximum perpendicular flux density on HTS coil is assumed 0.6 T, the critical current will decrease to 23 A. Here, the design algorithm is performed assuming that the field current is $I_f = 23$ A, but the flux density on HTS coil should be checked at the end.

The number of turns of field winding is calculated using equation (7) and assuming $I_f = 23$ A. due to winding limitations of HTS tapes, the HTS coils are usually formed by an especial shape that is known as pancake coil and is shown in Fig. 6. The height of each pancake coil is determined by width of HTS tape that is 3 mm according to Table II. In the same way, the width of pancake coils should be an integer coefficient of HTS wire thickness, i.e. 0.1 mm. On the other hand, the pancake coil width is limited by the space limitation between rotor poles. Therefore, the required turns of field winding should be provided by a few series pancakes. The pole height should be increased gradually until providing enough space for placing the stack of pancakes. After some try and error, eleven series pancakes that each of them contains 263 turns, form the winding of each rotor pole. The pancake formation was performed considering the critical bend diameter of SCS-3050 HTS wire.

TABLE II
HTS WIRE SPECIFICATIONS

| Parameters | Values | Unit |
|---|---|---|
| Critical current (at 77 K) | 75 | A |
| Width | 3 | mm |
| Thickness | 0.1 | mm |
| Critical tensile stress | > 550 | MPa |
| Critical bend diameter | 11 | mm |

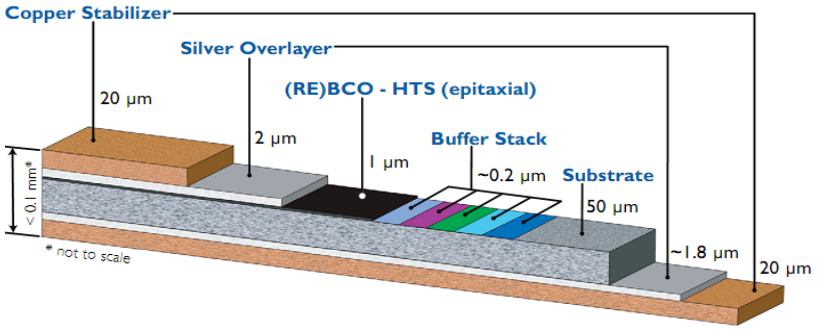


Fig. 4 HTS wire components and structure

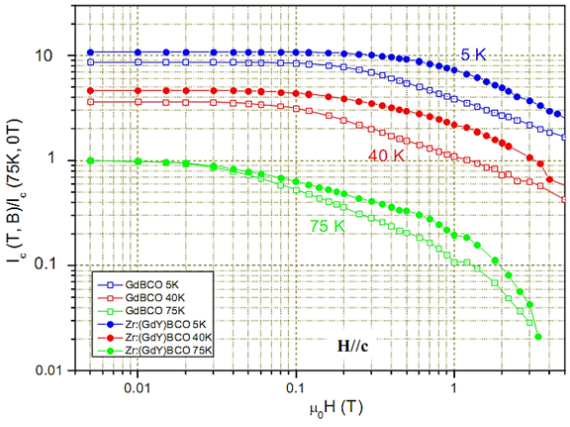


Fig. 5 Critical current characteristic of HTS wire

The flux diverter is made of magnetic material. The thickness of flux diverter differs in different parts and selected experimentally as a percentage of rotor yoke thickness, pole body arc, and pole shoe height.

Fig. 6 An example of pancake coils

*D.Cooling System Consideration*

Since the superconductivity occurs at very low temperature, the HTS coils must be cooled below a critical temperature by a cooling system. Several cooling systems are utilized for HTS machines that are mainly include the thermosyphon, open evaporative and piping evaporative [25]. Among these, the piping evaporative has better performance for large size and low speed HTS machines [25]. The cool rotor is isolated

against heat penetration and any rotor internal heat is collected by cooling pipes. These pipes carry the working fluid (liquid nitrogen) that transfers the rotor heat to outside the machine.

Design of complete cooling system in details is a voluminous work, which is outside the scope of this paper. In electromagnetic design stage, the cooling system type is selected, and its main requirements are considered. Here, the size of cooling pipes and the working fluid volume flow rate are considered regularly. The cooling pipes position is also proposed inside the flux diverters as shown in Fig. 7.

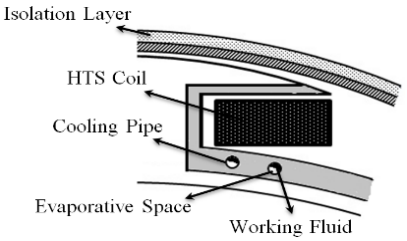


Fig. 7 Cooling system structure

*E. Stator Design*

It is necessary to design the stator winding in few parallel circuits due to the rather low voltage of armature. The number of pole pairs of rotor is a typical choice for the number of armature parallel circuits. By this assumption, the number of turns of armature winding per circuit is calculated as:

$$N_{ph} = \frac{2\pi . R_{is} . ac}{2m . I_{ph}} \tag{8}$$

Parameter $N_{ph}$ must be an integer coefficient of the number of slots per pole per phase, which is selected as $q = 5$ for the case study machine. To do this, the electrical loading factor is adjusted in an iterative loop according to Fig. 3.

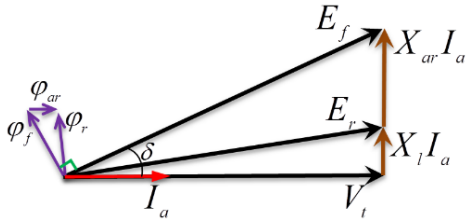


Fig. 8 Phasor-diagram of synchronous generator

In the proposed design algorithm, the machine axial length is calculated in this stage according to the required magnetic flux per pole ($\varphi_p$), which is a function of armature induced voltage ($E_a$). Parameter $E_a$ is selected as %3 larger than terminal voltage ($V_t$) to guarantee the unity power factor operation of the machine according to Fig. 8. The axial length of stator and rotor core can be calculated as:

$$L = \frac{\varphi_p}{(1 - k_{leak}) t_p . B_{tp}} \tag{9}$$

## IV. Final Design

The proposed algorithm is developed and run for designing a 1 MW synchronous generator. All dimensions are calculated. The rotor core consists of nonmagnetic mechanical support and U-shape flux diverters as shown in Fig. 9. The cooling pipes have been embedded in flux diverters, and are connected to the liaison rings in both sides of rotor core as shown in Fig. 10. A general scheme of machine's main part is shown in Fig. 11.

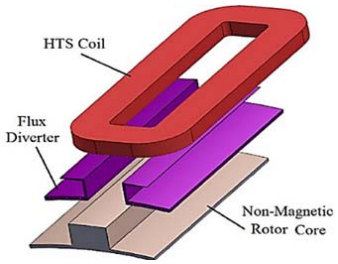


Fig. 9 Main component of a rotor pole

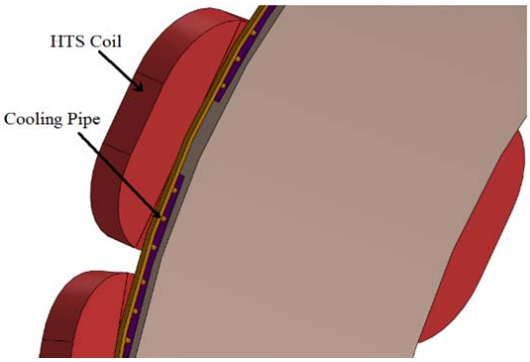


Fig. 10 Cooling pipes connection

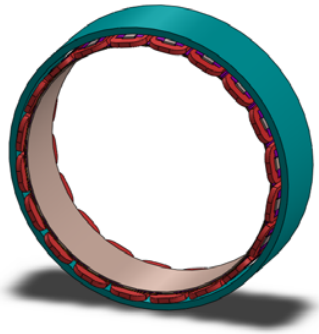

Fig. 11 General scheme of machine's main components

## V. FE Analysis

A 2D FE model of designed machine is developed to evaluate the electromagnetic performance of the machine. The

FE result of flux density distribution for a pairs of poles is shown in Fig. 12, which exhibits a good agreement with those results that calculated in design procedure. Furthermore, the maximum perpendicular flux density on HTS coil is obtained by FE model as shown in Fig. 13. The value of this parameter is estimated as $B_{\perp} = 0.54$ T, which is smaller than its maximum allowable value with a safety margin. The FE model is also developed to investigate the correctness of assumed value for leakage flux factor. This parameter is calculated as:

$$k_{leak} = 1 - \frac{\varphi_{st}}{\varphi_r} = 1 - \frac{0.0218}{0.0241} = 0.0903 \qquad (10)$$

which shows a good agreement with assumed value in (6). Winding loss and stator core loss are other parameters that are obtained by FE model. The efficiency of new machine is improved due to the stator core volume and consequently stator core loss decrement in addition to deletion the field winding loss. The volume of machine's active parts is decreased about %18 comparing to an ordinary similar size machine [21]. It is clear that the new machine is lighter than ordinary one.

## VI. Conclusion

The coreless rim-driven superconducting machine was developed in this paper as a new structure of superconducting hydraulic generator. The design algorithm of the new machine was developed and a 1 MW, 300 rpm rim-driven superconducting synchronous generator was designed for a hydraulic power plant, which exhibits superior advantages in weight, size, and efficiency comparing to an ordinary similar size synchronous generator. In addition, the rim-driven structure improves the hydrodynamic performance of the system. It seems that the new machine can be considered as an advanced structure of superconducting synchronous generators.

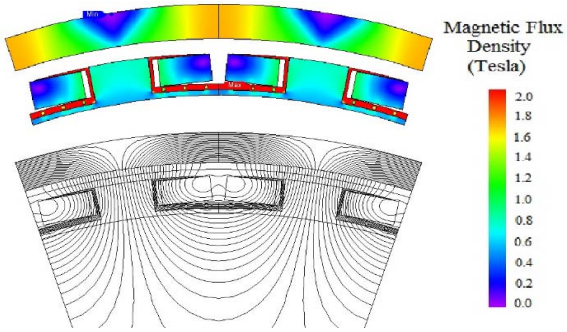


Fig. 12 Flux lines and Flux density distribution of a pairs of poles

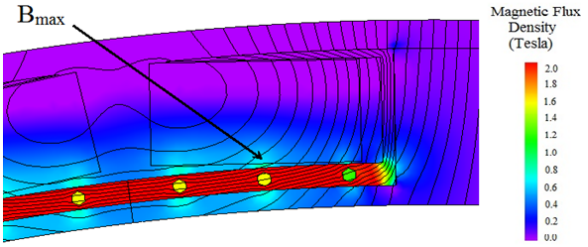


Fig. 13 Perpendicular component of flux density distribution over HTS coil

## References

[1] T. Nakamura, et al., "Fabrication and characteristics of HTS induction motor by the use of Bi-2223/Ag squirrel-cage rotor," IEEE Transactions on Applied Superconductivity, vol. 16, no. 2, pp. 1469-1372, 2006.
[2] M. Iwakuma, et al., "Development of a 15 kW motor with a fixed YBCO superconducting field winding," IEEE Transactions on Applied Superconductivity, vol. 17, no. 2, pp. 1607-1610, 2007.
[3] G. J. Barnes, M. McCulloch, and D. Dew-Hughes, "Applications and modelling of bulk HTS in brushless AC machines," Superconducting Science Technology, vol. 13, pp. 875-878, 2000.
[4] A. L. Rodrigues, "Drum and Disc Type Hysteresis Machines with Superconducting Rotors," in POWERENG 2009. Lisbon, Portugal: 2009.
[5] H. W. Neumuller, et al., "Advances in and prospects for development of high-temperature superconductor rotating machines at Siemens," Superconductor Science and Technology, vol. 19, pp. 114-117, 2006.
[6] E. N. Andreev, et al., "Development of high voltage superconductive alternator operating with DC transmission line," in 6th International Conference on Unconventional Electromechanical and Electrical Systems UEES04, Alushta, Ukraine: 2004, pp. 945-950.
[7] Xiaohang Li et al., "Design of a High Temperature Superconducting Generator for Wind Power Applications", IEEE Transactions on Applied Superconductivity, vol. 21, no. 3, pp. 1155-1158, 2011.
[8] Di Wu, and Edward Chen, "Stator Design for a 1000 kW HTSC Motor With Air-gap Winding", IEEE Transactions on Applied Superconductivity, vol. 21, no. 3, pp. 1093-1096, 2011.
[9] Satoshi Fukui, Jun Ogawa, Takao Sato, Osami Tsukamoto, Naoji Kashima, and Shigeo Nagaya, "Study of 10 MW-Class Wind Turbine Synchronous Generators With HTS Field Windings", IEEE Transactions on Applied Superconductivity, vol. 21, no. 3, pp. 1151-1154, 2011.
[10] Wendell Bailey, Huaming Wen, Maitham Al-Mosawi, Kevin Goddard, and Yifeng Yang, "Testing of a Lightweight Coreless HTS Synchronous Generator Cooled by Subcooled Liquid Nitrogen", IEEE Transactions on Applied Superconductivity, vol. 21, no. 3, pp. 1159-1162, 2011.
[11] K. F. Goddard, B. Lukasik, and J. K. Sykulski, "Alternative Designs of High-Temperature Superconducting Synchronous Generators", IEEE Transactions on Applied Superconductivity, vol. 19, no. 6, pp. 3805-3811, 2009.
[12] Rolls-Royce marine propulsion products. 2004; Available online: www.rolls-royce.com/marine.
[13] O. Krovel, R. Nilssen, S. E. Skaar, E. Løvli and N. Sandoy, "Design of an integrated 100kW Permanent Magnet Synchronous Machine in a Prototype Thruster for Ship Propulsion," in Proc. ICEM2004, Cracow, Poland: 2004, pp. 117-123.
[14] S. H. Lai, "Design Optimisation of a Slotless Brushless Permanent Magnet DC Motor with Helically-Wound Laminations for Underwater Rim-Driven Thrusters", Ph.D. dissertation, Facul. Eng. Sci. and Math., Univ. of Southampton, Southampton, UK, 2006.
[15] P. M. Tuohy, A. C. Smith and M. Husband, "Induction rim-drive for a marine propulsor," in 5th IET International Conference on Power Electronics, Machines and Drives, Brighton, UK: 2010.
[16] S. Djebarri, J. F. Charpentier, F. Sculiller, M. Benbouzid and S. Guemard, "Rough Design of a Double-Stator Axial Flux Permanent Magnet Generator for a Rim-Driven Marine Current Turbine," in Proc. ISIE IEEE International Symposium on Industrial Electronics, Hangzhou, 2012, pp. 1450-1455.
[17] C. Pashias, and S.R. Turnock, "Hydrodynamic design of bi-directional, rim-driven ducted thruster siutable for underwater vehicles," in Ship Science Report, No. 128, 2003.

[18] Q. Krovel, "Design of Large Permanent Magnetized Synchronous Electric Machines," PhD Thesis, Norwegian University of Science and Technology: Trondheim. 2011.
[19] S. M. Sharkh, and S.H. Lai, "Slotless PM Brushless Motor With Helical Edge-Wound Laminations," IEEE Transactions on Energy Conversion, vol. 21, no. 3, pp. 594-598, 2009.
[20] China Suplier, "1000kw 250rpm Permanent Magnet Generator", Available online: http://njlewis.en.made-in-china.com.
[21] H. M. Kim, Y. S. Yoon, Y. K. Kwon, Y. C. Kim, S. H. Lee, J. P. Hong, J. B. Song, and H. G. Lee, "Design of Damper to Protect the Field Coil of an HTS Synchronous Motor," IEEE Transactions on Applied Superconductivity, vol. 19, no. 3, pp. 1683-1686, 2009.
[22] Y. S. Jo, et al., "High Temperature Superconducting Synchronous Motor," IEEE Transactions on Applied Superconductivity, vol. 12, no. 1, pp. 833-836, 2002.
[23] SuperPower 2G HTS Wire Specifications. Super Power Inc., Schenectady, NY, USA, Available online: www.superpower-inc.com/system/files/SP_2G+Wire+Spec+Sheet_for+web_2013FEC_v2_0.pdf.
[24] D. Hazelton, and T. Lehner, 2010, SuperPower 2G HTS Wire for Electrical and Magnet Applications, Available online: indico.cern.ch/materialDisplay.py?materialId=slides&confId=96071.
[25] B. Chen, G. B. Gu, G. Q. Zhang, F. C. Song, and C. H. Zhao, "Analysis and Design of Cooling System in High Temperature Superconducting Synchronous Machines," IEEE Transactins on Applied Superconductivity, vol. 17, no. 2, pp. 1557-1560, 2007.

**A. Hassannia** was born in Gonabad, Iran, on February 1984. He received the B.Sc. degree from the Ferdowsi University of Mashhad, Mashhad, Iran, in 2006, and the M.Sc. and Ph.D. degrees from the Faculty of Electrical and Robotic Engineering, Shahrood University of Technology, Shahrood, Iran, in 2008 and 2013 respectively, both in electrical engineering. He is currently with the Shahrood University of Technology as assistant professor. His research interests include design and modeling of electrical machines, superconducting motors and fuzzy control.

**S. Ramezani** Received the B.Sc and M.Sc. degrees from the Noshirvani University of Technology and Shahrood University of Technology respectively, both of them in power electrical engineering. She is now the lecture with the Sim & Kabl Moghan University, Shahrood, Iran.